Springer

KSME

Journal of Mechanical Science and Technology 27 (8) (2013) 2557~2568
www.springerlink.com/content/1738-494x
DOI 10.1007/s12206-013-0640-7

Modeling and numerical simulation of a pilot-stabilized turbulent premixed flame †

Abdallah Benarous[1,2,*], Djamel Karmed[3] and Abdelkrim Liazid[2]

[1]*Department of Mechanical Engineering, Hassiba Benbouali University, Chlef, Algeria*
[2]*LTE Laboratory, National Polytechnic School (ENP), Oran, Algeria*
[3]*Thermal and Combustion Section, Pprime Institute, Poitiers University, Chasseneuil Cedex, France*

(Manuscript Received November 18, 2012; Revised March 3, 2013; Accepted April 9, 2013)

Abstract

The present paper is devoted to the numerical modeling of turbulent reactive flows subjected to spatial variations of equivalence ratio. In such situations, the description of the local thermochemistry requires at least two variables. The mixture fraction and the fuel mass fraction are respectively chosen to describe the composition of the fresh mixture and the chemical reaction progress. In the present contribution, a generalization of the Libby-Williams (LW) approach to four delta probability density function (Pdf) is presented. Transport equations for the first and second-order (variance) of mean scalar quantities are numerically solved. Moreover, the so-called LW-P model solves an additional transport equation for the cross-correlation between the reactive and the passive scalars. The model is applied to the calculation of a turbulent lean-premixed flow of methane and air stabilized by a near-stoichiometric pilot-flame. Numerical results regarding flow dynamics and flame structure are compared with the experimental data of a laboratory-scale burner-chamber device.

Keywords: Fuel mass fraction; Libby-Williams-Poitiers model; Mixture fraction; Partially premixed combustion; Reactive flows

1. Introduction

Lean premixed combustion remains as one of the most important technologies for achieving an ultra low NOx and high fuel economy combustion system without having an adverse effect on the combustion efficiency [1]. However, lean premixed configurations are more sensitive to external perturbations yielding to so-called flame instabilities. In this context, co-flows of air or pilot- flames are widely used to stabilize the premixed flame and to help maintaining continual combustion far from critical points of the system. In many applications, such as gas turbines for land-based power generation as well as industrial burners, it is difficult to ensure a complete mixing of the fuel and air before combustion starts. Space and time available for mixing are often severely constrained by overall considerations of size and weight. Moreover, for stability and ignitability considerations, it is important that co-flows of air or flue gases operate at different richness from those of the main flows [2]. Accordingly the equivalence ratio of the mixture is a space and time variable and combustion occurs in the form of partially premixed flames. In this situation, the characteristic Damköhler number (τ_{turb}/τ_{chem}) cannot always be considered as infinite and combustion may extend from thin flamelets regime to thickened flame regime. A number of experiments have been done to study the effect of stratification on flame structure [3], flame propagation speed [4, 5] and flame brush thickness [6, 7]. In the same context, various Reynolds averaged numerical simulations (RANS) have been carried out to evaluate the influence equivalence ratio gradients on heat release rates [8] and emission levels [9]. Recently stratification effects on CO and NO emissions have been evidenced by means of large eddy simulations (LES) [10] and direct numerical simulations (DNS) [11].

For partially premixed combustion, most of models are mainly based on approaches such as coherent flame modeling [12], flame surface density [13] and presumed probability density functions (Pdf) [14]. The most attractive among the proposed models is the presumed Pdf variety which offers a combination of simplicity, reduced computational cost and reasonable accuracy. However, there are several issues that arise including the shape of the Pdf, the statistical dependence of the variables and the closure of the scalar terms which appear in the transport equations of second moment quantities [15]. In fully premixed situations where the thermochemistry is described by only one variable, the Libby-Williams (LW) model based on two-Dirac delta functions [16] has demonstrated its ability to recover both thin and thickened flame regimes. The generalization of the LW model to partially premixed conditions was introduced by Robin et al. [17]. These authors introduced a multi-Dirac Pdf function to account for situations where gradients of equivalence ratio are encoun-

*Corresponding author. Tel.: +21 327721794, Fax.: +21 327725832
E-mail address: a.benarous@univ-chlef.dz
† Recommended by Editor Oh Chae Kwon

Table 1. Validation cases for the LW-P model.

Flame geometry	Planar 2D	Planar 2D	V shaped	Conical-shaped
Stabilization	Bluff body	Sudden expansion	Circular rod	Pilot flame
Number of incoming streams	2	2	1	2
Streams type	Products / products CO_2, H_2O	Reactants / reactants propane, air	Reactants propane, air	Reactants / products methane, air / CO_2, H_2O
Equivalence ratio Φ	Φ(1) = 0.8 Φ(2) = 0.8	Φ(1) = 0.8 Φ(2) = 0.9	Φ = 0.65 → Φ = 0.80	Φ(1) = 0.6 Φ(2) = 1.03
References	Ribert et al. [18]	Robin et al. [17]	Robin et al. [19]	Present study

tered. The so-called LW-P model (Libby-Williams-Poitiers) uses the mixture fraction and the fuel mass fraction to describe both mixing and reaction progress. The application of the LW-P model has been successfully carried out for the description of a reactive shear layer stabilized by parallel incoming streams of hot products with equal equivalence ratios [18]. Robin et al. [17] have performed RANS calculations to reproduce the structure of two flames stabilized by a 2D sudden expansion. The premixed flames were established from two fresh mixtures with slightly different equivalence ratios. The authors also succeed in validating the LW-P model against the experimental data of a stratified V-shaped flame [19]. Table 1 depicts a summary of the validation cases for the LW-P model. As stated above, the LW-P model has been validated on various partially premixed configurations witnessing slight gradients of equivalence ratio.

In the present investigation turbulent partially premixed combustion is studied in the special case where a strong mean gradient of equivalence ratio exists. In this respect, a new closure expression for the scalar variances is used to interpolate between thin flamelets and thickened flame regimes. The paper is organized as follows: after a general description of the two-scalar thermochemical state in a partially premixed situation, the mathematical formulation of the LW-P model is presented. In a second step, the experimental data of the ICARE burner [5, 7] are used to test the ability of the LW-P model to deal with high varying stoichiometry conditions. RANS calculation is performed in both non-reactive and reactive cases. The mathematical formulation of the standard ($k-\varepsilon$) turbulence model is slightly modified to account for round jet effects encountered in the experimental configuration. Numerical results regarding turbulent mixing and flame structure are confronted with the available experimental data.

2. Thermochemical state

The complete reaction of methane is idealized as:

$$CH_4 + 2(O_2 + 3.76N_2) \rightarrow CO_2 + 2H_2O + 7.52N_2 \,. \quad (1)$$

Following the analysis of Libby et al. [16], we identify the element mass fractions as $Z_1 \rightarrow O_2; Z_2 \rightarrow H_2; Z_3 \rightarrow C$ and the species mass fractions as $Y_1 \rightarrow O_2; Y_2 \rightarrow CH_4; Y_3 \rightarrow H_2O; Y_4 \rightarrow CO_2; Y_5 \rightarrow N_2$ Balance equations are written as:

$$\begin{aligned} Z_1 &= Y_1 + \mu_{13}Y_3 + \mu_{14}Y_4 \\ Z_2 &= \mu_{22}Y_2 + \mu_{23}Y_3 \\ Z_3 &= \mu_{32}Y_2 + \mu_{34}Y_4 \\ Y_5 &= 1 - Z_1 - Z_2 - Z_3 \end{aligned} \quad (2)$$

where μ_{ij} is the number of grams of element i in species j. It should be stressed that in a specified mixture of methane and air, the element mass fractions Z_i are known (with respect to a prescribed equivalence ratio Φ) and the associated element mass fractions are likewise known. For a fresh mixture, the products are assumed absent, so that:

$$\begin{aligned} Z_1 &= Y_1 \\ Z_2 &= \mu_{22}Y_2 \\ Z_3 &= \mu_{32}Y_2 \\ Y_5 &= 1 - Z_1 - Z_2 - Z_3 \\ Y_3 &= Y_4 = 0 \,. \end{aligned} \quad (3)$$

In the same way, when considering a complete combustion, the composition for both fuel-rich and fuel-lean considerations in the burnt mixture is respectively given by:

$$\begin{aligned} Y_1 &= 0 \\ Y_2 &= \frac{(\mu_{13}/\mu_{23})Z_2 + (\mu_{14}/\mu_{34})Z_3 - Z_1}{(\mu_{13}\mu_{22}/\mu_{23}) + (\mu_{32}\mu_{14}/\mu_{34})} \\ Y_3 &= \frac{Z_2 - \mu_{22}Y_2}{\mu_{23}} \\ Y_4 &= \frac{Z_3 - \mu_{32}Y_2}{\mu_{34}} \end{aligned} \quad (4)$$

and

$$\begin{aligned} Y_1 &= Z_1 - \frac{\mu_{13}}{\mu_{23}}Z_2 - \frac{\mu_{14}}{\mu_{34}}Z_3 \\ Y_2 &= 0 \\ Y_3 &= \frac{Z_2}{\mu_{23}} \\ Y_4 &= \frac{Z_3}{\mu_{34}} \,. \end{aligned} \quad (5)$$

More generally, with the set of Eq. (2), all the species mass fractions provide the fraction of one species. In our case, Y_2 the mass fraction of fuel (denoted Y in the following) is taken to be that determining species.

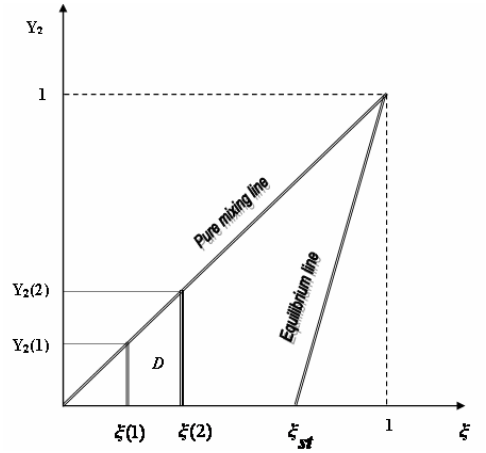

Fig. 1. Domain of definition in the composition space.

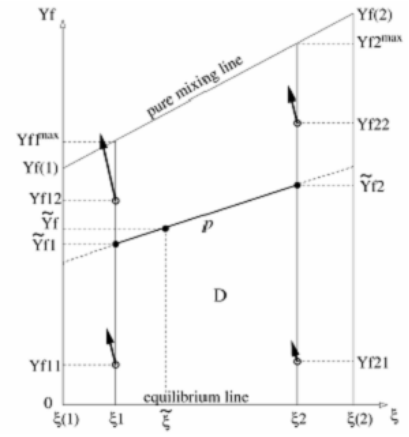

Fig. 2. Locations of the four delta functions in the domain *D*.

If we follow the practice relevant to analyses of non pre-mixed combustion, one introduces a conserved scalar ξ in such a fashion that $\xi = 0$ in the pure air stream and $\xi = 1$ in the fuel stream.

The following definition of the mixture fraction is used:

$$\xi = (Y_5 - Y_5^{\min})/(Y_5^{\max} - Y_5^{\min}) \tag{6}$$

where superscripts min and max correspond to pure air and fuel, respectively. If the radiative heat transfer is neglected and the walls are adiabatic, the time dependent transport equations for ξ and the enthalpy of the mixture, are identical [20]. Consequently, our definition of the fuel mass fraction Y (Eq. (2)) and the mixture fraction helps in the determination of the entire time and space state of the mixture. Thus we deal with a two scalar thermochemical system.

3. Description of the LW-P model

In the space coordinate (Y, ξ), the domain of definition is limited by two vertical lines $\xi = \xi(1)$ and $\xi = \xi(2)$. The pure mixing line corresponds to the mixing between these two streams without combustion (Fig. 1). It must be noticed that in this specific case, these two limits are never reached and ξ stays in the range $\xi(1) \le \xi \le \xi(2)$. The extreme situation where $0 \le \xi \le 1$ would correspond to a non-premixed flame.

3.1 Dynamic field modeling

Favre averaged form for each extensive quantity (except pressure and density) is considered leading to the following mean equations of continuity and momentum:

$$\begin{aligned} &\frac{\partial \bar{\rho}}{\partial t} + \frac{\partial \bar{\rho} \tilde{u}_k}{\partial x_k} = 0 \\ &\frac{\partial \bar{\rho} \tilde{u}_k}{\partial t} + \frac{\partial \bar{\rho}\, \tilde{u}_k \tilde{u}_j}{\partial x_j} + \frac{\partial \bar{p}}{\partial x_k} = -\frac{\partial}{\partial x_j}(\overline{\rho\, u_k'' u_j''} - \overline{\tau_{kj}}) . \end{aligned} \tag{7}$$

In the previous set of equations, body forces and radiation fluxes have been neglected.

Turbulent fluxes of velocity are closed using the viscosity assumption:

$$\overline{\rho\, u_k'' u_j''} = -\mu_T \left(\frac{\partial \tilde{u}_k}{\partial x_j} + \frac{\partial \tilde{u}_j}{\partial x_k} - \frac{2}{3}\delta_{kj}\frac{\partial \tilde{u}_i}{\partial x_i}\right) \tag{8}$$

where μ_T is the turbulent viscosity, given by:

$$\mu_T = C_\mu \bar{\rho}\, \tilde{k}^2 / \tilde{\varepsilon} . \tag{9}$$

The previous system is completed by the transport equations of the turbulent kinetic energy $\tilde{k}$ and its dissipation rate $\tilde{\varepsilon}$ [21].

3.2 Reaction rate modeling

One introduces a mass-weighted joint Pdf of ξ and Y made of four Dirac delta functions, as:

$$\begin{aligned} &\tilde{P}(\xi, Y) = \alpha \tilde{P}_1(Y)\delta(\xi - \xi_1) + \\ &(1-\alpha)\tilde{P}_2(Y)\delta(\xi - \xi_2) . \end{aligned} \tag{10}$$

$\tilde{P}_1, \tilde{P}_2$ are the two conditional Pdf at $\xi = \xi_1$ and $\xi = \xi_2$, defined as:

$$\begin{aligned} \tilde{P}_1(Y) &= \beta\delta(Y - Y_{11}) + (1-\beta)\delta(Y - Y_{12}) \\ \tilde{P}_2(Y) &= \gamma\delta(Y - Y_{21}) + (1-\gamma)\delta(Y - Y_{22}) \end{aligned} \tag{11}$$

where $\alpha, \beta, \gamma, \xi_1, \xi_2, Y_{ij}$ are the nine Pdf parameters depending on the location inside the flow field (Fig. 2). The above parameters are determined according to the procedure de-

scribed by Robin et al. [17].

The Pdf shape allows for the evaluation of the mean chemical rate $\bar{\omega}$:

$$\bar{\omega} = \bar{\rho}\iint_D \frac{\omega(\xi,Y)}{\rho(\xi,Y)}\tilde{P}(\xi,Y)d\xi dY \tag{12}$$

where D is the space definition domain of the Pdf. In the present model we consider only a global one-step reaction so that the rate of fuel consumption ω is written as [22]:

$$\omega(\xi,Y) = \rho(\xi,Y).B(\xi)\left(Y - Y_{\min}\right)\exp\left(-T_a / T\right) \tag{13}$$

where $T_a = 20{,}000K$ is the activation temperature and $Y_{\min} = 0$ in the case of a lean mixture. The pre-exponential factor $B(\xi)$ is assumed depending on the equivalence ratio. A look-up table $B(\xi(\Phi))$ can be obtained by means of a laminar chemistry calculation [19].

3.3 Scalar transport equations

To provide a closed system, five balance equations, i.e., those for the first- and second- order scalar quantities are needed:

$$L(\tilde{\xi}) = 0 \tag{14}$$

$$L(\tilde{Y}) = \bar{\omega} \tag{15}$$

$$L(\frac{\overline{\rho\xi^{"2}}}{\bar{\rho}}) = -2\tilde{\chi}_\xi - 2\overline{\rho.\mathbf{u}^{"}\xi^{"}}.\nabla\tilde{\xi} \tag{16}$$

$$L(\frac{\overline{\rho Y^{"2}}}{\bar{\rho}}) = -2\tilde{\chi}_Y - 2\overline{\rho.\mathbf{u}^{"}Y^{"}}.\nabla\tilde{Y} + 2\overline{Y^{"}\omega} \tag{17}$$

$$L(\frac{\overline{\rho Y^{"}\xi^{"}}}{\bar{\rho}}) = -2\tilde{\chi}_{\xi Y} - \overline{\rho.\mathbf{u}^{"}Y^{"}}.\nabla\tilde{\xi} + \\ -\overline{\rho.\mathbf{u}^{"}\xi^{"}}.\nabla\tilde{Y} + \overline{\xi^{"}\omega} \tag{18}$$

where L is a mean convection-diffusion operator defined as:

$$L(\tilde{g}) = \frac{\partial}{\partial t}(\bar{\rho}\tilde{g}) + \nabla.(\bar{\rho}\,\tilde{\mathbf{u}}\tilde{g}) - \nabla.(\overline{\rho D\,\nabla g} - \overline{\rho\,\mathbf{u}^{"}g^{"}}) \tag{19}$$

and $\tilde{\chi}_\xi$, $\tilde{\chi}_Y$, $\tilde{\chi}_{\xi Y}$ are the mean dissipation terms due to molecular diffusion.

The terms $\bar{\omega}, Y^{"}\omega, \xi^{"}\omega$ are related to chemical production of the fuel mass fraction Y and are expressed by means of finite sums over the peaks of the Pdf [17]. In the present paper, a first-order version of the LW-P model is used to close the turbulent scalar fluxes using a gradient approximation:

$$\overline{\rho u_k^{"}\xi^{"}} = -\bar{\rho}D_T\frac{\partial\tilde{\xi}}{\partial x_k} \tag{20}$$

$$\overline{\rho u_k^{"}Y^{"}} = -\bar{\rho}D_T\frac{\partial\tilde{Y}}{\partial x_k} \tag{21}$$

where $D_T = C_\mu\tilde{k}^2 / Sc_T\tilde{\varepsilon}$ is the turbulent diffusion coefficient and $C_\mu = 0.09$. Sc_T is the turbulent Schmidt number set to its usual value 0.7.

It must be noticed here that such approximation cannot predict flame-generated turbulence that may be associated to countergradient diffusion [23].

3.4 Scalar dissipation terms

The mean dissipation terms which appear in the transport Eqs. (16)-(18) represent the mean mixing rate at small scales. The modeling of the three scalar dissipation rates $\tilde{\chi}_\xi = \overline{2\rho D\frac{\partial\xi^{"}}{\partial x_k}\frac{\partial\xi^{"}}{\partial x_k}}$, $\tilde{\chi}_Y = \overline{2\rho D\frac{\partial Y^{"}}{\partial x_k}\frac{\partial Y^{"}}{\partial x_k}}$ and $\tilde{\chi}_{\xi Y} = \overline{2\rho D\frac{\partial\xi^{"}}{\partial x_k}\frac{\partial Y^{"}}{\partial x_k}}$ is one of the most challenging problems in the description of partially premixed systems.

In the LW-P model, the dissipation rate $\tilde{\chi}_\xi$ of the mixture fraction is based on an analogy with turbulent mixing:

$$\tilde{\chi}_\xi = R\left(\tilde{\varepsilon}/\tilde{k}\right)\overline{\rho\xi^{"2}} \tag{22}$$

where the constant R is close to 2 [24].

This closure expression has been shown to work well for passive scalars. This is not the case for a reactive scalar since it is believed to be influenced by turbulence and chemistry coupling. In order to recover the two limiting flame regimes, namely the thickened flames ($\tau_{chem} << \tau_{turb}$) and the thin flamelets ($\tau_{chem} >> \tau_{turb}$), a linear bridging methodology is used for the following expressions of the scalar dissipation rates [25]:

$$\tilde{\chi}_Y = 2\bar{\rho}\left(S\,\tilde{\in}_Y + \left(1-S\right)R\left(\frac{\tilde{\varepsilon}}{\tilde{k}}\right)\frac{\overline{\rho Y^{"2}}}{\bar{\rho}}\right) \tag{23}$$

$$\tilde{\chi}_{\xi Y} = 2\bar{\rho}\left(S\,\tilde{\in}_{\xi Y} + \left(1-S\right)R\left(\frac{\tilde{\varepsilon}}{\tilde{k}}\right)\frac{\overline{\rho Y^{"}\xi^{"}}}{\bar{\rho}}\right). \tag{24}$$

The segregation factor S is defined as:

$$S = \frac{\overline{\rho Y^{"2}}}{\left(\overline{\rho Y^{"2}}\right)_{\max}} \tag{25}$$

and $\left(\overline{\rho Y^{"2}}\right)_{\max} = \bar{\rho}\left(\tilde{Y}_{\max} - \tilde{Y}\right)\left(\tilde{Y}\right) + \left(\theta\right)\frac{\overline{\rho\xi^{"2}}}{\bar{\rho}}$. (26)

For lean mixtures θ is defined as $\theta = \left(\tilde{Y}\right)/\left(\tilde{Y}_{\max}\right)$ and $\tilde{Y}_{\max}$ is defined by the bounds of the composition space.

Details on closure expressions for the mean dissipation rates

of the fuel mass fraction variance and the cross correlation variance $\tilde{\epsilon}_Y, \tilde{\epsilon}_{\xi Y}$ can be found in Mura et al. [25].

4. Description of the ICARE facility

The stainless steel cylindrical high pressure combustion chamber of ICARE (Orléans, France) can sustain premixed flames up to 1 MPa [7]. The chamber consists of two cylindrical halves of 600 mm high and 300 mm inner diameter. Each halve contains four windows of 100 mm diameter designed for the optical diagnostics. The burner with 25 mm diameter is placed in the centre of the chamber and can be moved along the vertical axis by means of a stepping motor. The upper part of the burner has a convergent profile.

A porous grid is placed in the bottom part of this burner section to homogenize the turbulence field at the inlet of the combustion chamber (Fig. 3(a)). The grid is a circular perforated plate with a mesh size M = 3.1 mm and a hole diameter d = 2.5 mm (Fig. 3(b)).The main flame consists of a lean methane-air mixture with an equivalent ratio of 0.6. It is surrounded by a 2 mm laminar pilot flame at near-stoichiometric conditions. For the non reactive case, the measurements have evidenced an isotropic character of the turbulence in the downstream of the axial station X = 5 mm. Here, axial velocity and turbulent kinetic energy were measured in five radial locations (r = *0* mm to r = 12.5 mm).

On the other hand, the reactive measurements were mainly carried out along the chamber centerline (r = *0*) up to the axial station X = 137.5 mm. Owing to the apparition of flash-back situations, the flow rate and the stoichiometry of the pilot flame were experimentally adjusted in such a fashion that the main flame remains attached to the burner while keeping a conical shape (Fig. 3(c)).

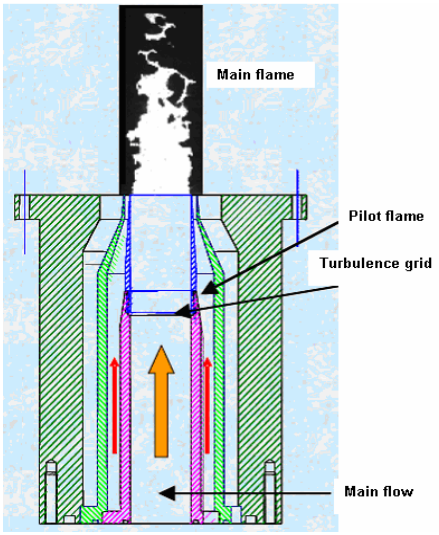

(a) ICARE burner

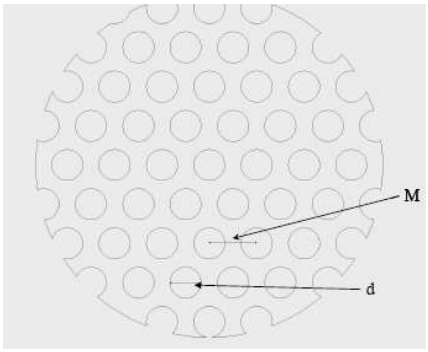

(b) Turbulence grid

(c) Bunsen flame.

Fig. 3. Schematic view.

5. Results and discussions

5.1 The numerical procedure

The LW-P model has been implemented in the computational fluid dynamic software Code_Saturne [26]. The solver allows parallel calculations based on a finite volume method.

Favre averaged forms of the Navier-Stokes equations are numerically solved additionally with equations for additional scalars (species concentration and possible user-defined scalars). The operating scheme is based on a prediction of the velocity field followed by a pressure correction step. The CFD code makes it possible to perform LES simulations, but in the present paper, only RANS calculations with a two-equation ($k-\varepsilon$) model are used. A structured mesh has been generated to represent half of the physical domain (Fig. 4).

A local refinement was operated in a thin region located in the interface between the main stream and the co-flow. The retained grid containing approximately 76000 cells has been obtained from several numerical tests. Finer meshes did not influence the centerline static temperature by more than 5% (Fig. 5).

5.2 The boundary conditions

Inlet boundary conditions must be handled with special care, since they may have a strong influence on the combustion development inside the computational domain. This is often complicated by several constraints. Firstly, experimental measurements of velocity and turbulent kinetic energy are only available from 5 mm downstream the inlet of the compu-

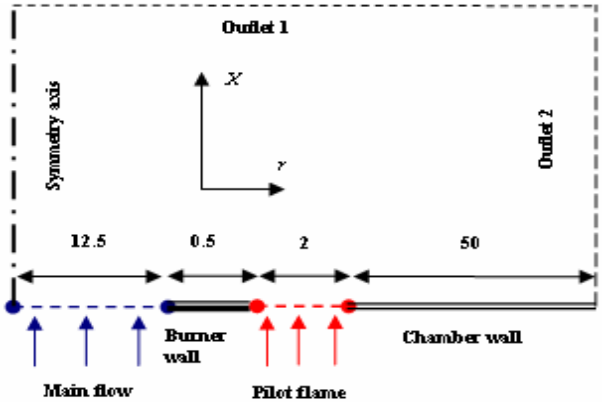

Fig. 4. The computational domain (axisymmetric).

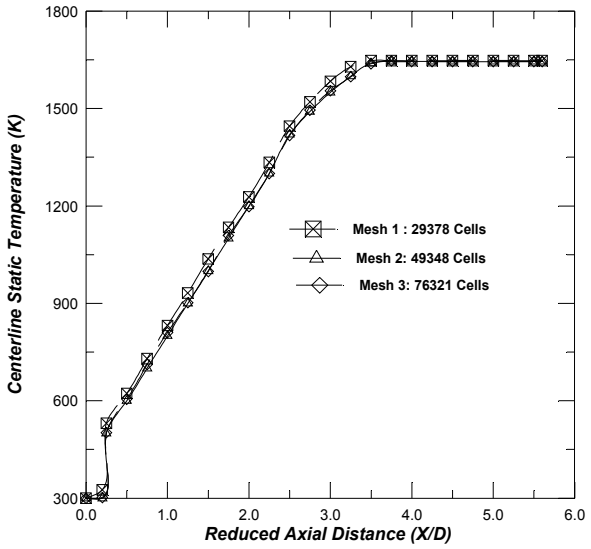

Fig. 5. Grid sensitivity study based on centerline static temperature.

tational domain [5, 7]. Secondly, there was a lack of data regarding the radial evolution of the dissipation rate at the same position. Owing to the previous difficulties, a preliminary calculation has been performed on the non reactive flow within the burner. Here, bulk values for the velocity and turbulent intensity have been used as boundary conditions at the burner inlet. The values were related to the operating flow rate of the burner and the characteristics of the turbulence grid [5]. At the burner exit, a power law for the radial profile (Fig. 6(a)) of the axial velocity is adopted:

$$u(r) = u_0(1 - r/r_b)^n \,. \tag{27}$$

In Eq. (27) r_b denotes the burner radius, u_0 is the centerline velocity and $n = 0.2818$. In the same way, profile of the turbulent kinetic energy was approximated by a second order polynomial expression:

$$k(r) = k_0 + a_1 r + a_2 r^2 \,. \tag{28}$$

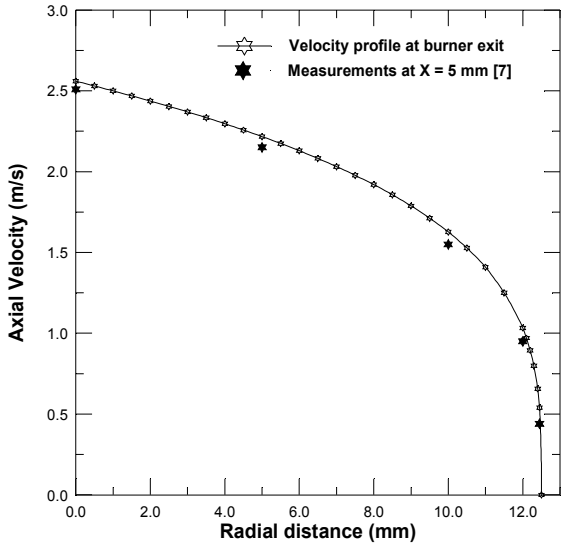

(a)

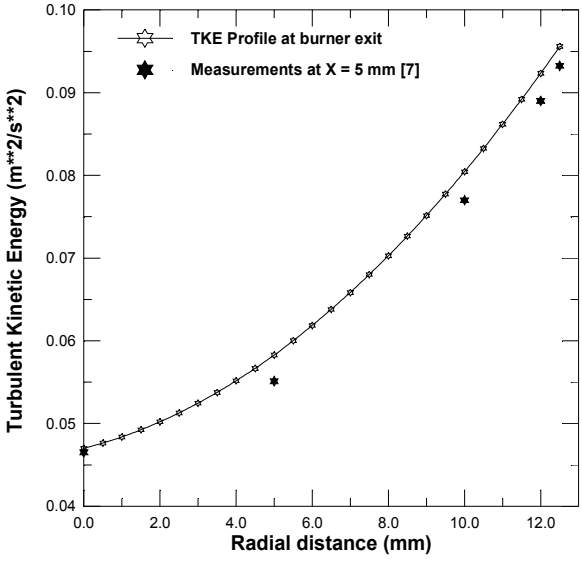

(b)

Fig. 6. (a) Boundary condition for the axial velocity; (b) Boundary condition for the turbulent kinetic energy.

a_1, a_2 stand for the constants of the interpolation and $k_0 = 0.047\ \mathrm{m^2/s^2}$ is the centerline value of the turbulent kinetic energy (Fig. 6(b)). Regarding the dissipation rate ε, the derivation of the profile expression was based upon a constant value $L_t = 2.9$ mm of the turbulence length scale.

As stated out by Pavé [5], this value is expected to be close to the size of the turbulence grid mesh. In the present study, the pilot flame was modeled as a co-flow of flue gases being burned at near-stoichiometric conditions. In order to avoid disturbing the main flame while preserving the laminar character of the co-flow, bulk values for the velocity and turbulent intensity were chosen to be as low as possible. Numerical values for the co-flow boundary conditions depicted in Table 2, have allowed a stabilization of the main flame.

Table 2. Boundary conditions specification.

	Main flow	Co-flow
Velocity (m/s)	$u_0 = 2.56$	$0.05u_d$
k (m^2/s^2)	r^2 polynomial	$k = k(I = 5\%)$
ε (m^2/s^3)	r^3 polynomial	$\varepsilon = \varepsilon(I = 5\%)$
T (K)	300	$T(\xi_{st})$
Equivalence ratio	0.6	1.03

5.3 The non reactive case

As a first step, it is interesting to perform a non-reactive flow calculation. The so-called "cold flow simulation" helps to choose the appropriate turbulence model describing the mixing and tune the empirical constants. Moreover, solving the scalar transport equations without chemical source terms provides a "guess" solution field for the reactive calculations. According to the mathematical form implemented in Code_Saturne solver, the standard ($k-\varepsilon$) model has been proven to be efficient for planar flows [25]. The model is not suited for 3D or axisymmetric configurations where round jet effects are present. To account for vortex stretching occurring in three-dimensional flows, a Pope correction [27] has been implemented in the Code_Saturne solver. The non-dimensional measure of a vortex stretching is the invariant χ defined as:

$$\chi = W_{ij}W_{jk}S_{ki} \tag{29}$$

where:

$$S_{ij} = \frac{1}{2}\frac{\tilde{k}}{\tilde{\varepsilon}}\left(\frac{\partial \tilde{u}_i}{\partial x_j} + \frac{\partial \tilde{u}_j}{\partial x_i}\right), W_{ij} = \frac{1}{2}\frac{\tilde{k}}{\tilde{\varepsilon}}\left(\frac{\partial \tilde{u}_i}{\partial x_j} - \frac{\partial \tilde{u}_j}{\partial x_i}\right). \tag{30}$$

Pope [26] stated that the dissipation source is an increasing function of χ and therefore can be represented by a linear expression. Hence, the modified transport equation for the dissipation rate $\tilde{\varepsilon}$ can be written as [27]:

$$\frac{D}{Dt}(\bar{\rho}\,\tilde{\varepsilon}) = \frac{\partial}{\partial x_i}\left(\frac{\mu_T}{\sigma_\varepsilon}\frac{\partial(\bar{\rho}\,\tilde{\varepsilon})}{\partial x_i}\right) + \\ + \frac{\tilde{\varepsilon}}{\tilde{k}}(C_{1\varepsilon}P - C_{2\varepsilon}\tilde{\varepsilon}.\bar{\rho} + C_{3\varepsilon}\tilde{\varepsilon}.\bar{\rho}\chi) \tag{31}$$

where $C_{3\varepsilon}$ is a positive constant and P is the production rate of the turbulent kinetic energy. Commonly used values for the constants $C_{1\varepsilon}, C_{3\varepsilon}, \sigma_\varepsilon$ are 1.45, 0.84 and 1.3, respectively.

According to several numerical tests the value $C_{2\varepsilon} = 1.84$ has allowed for a quite good agreement between the axial velocity and the centerline measurements.

Figs. 7 and 8 show respectively the centerline profiles of the mean velocity component $\tilde{u}$ and the turbulent kinetic energy $\tilde{k}$. A quasi-linear decrease is observed on the velocity profile until $X_c = 78$ mm where a slope change occurs (Fig. 7).

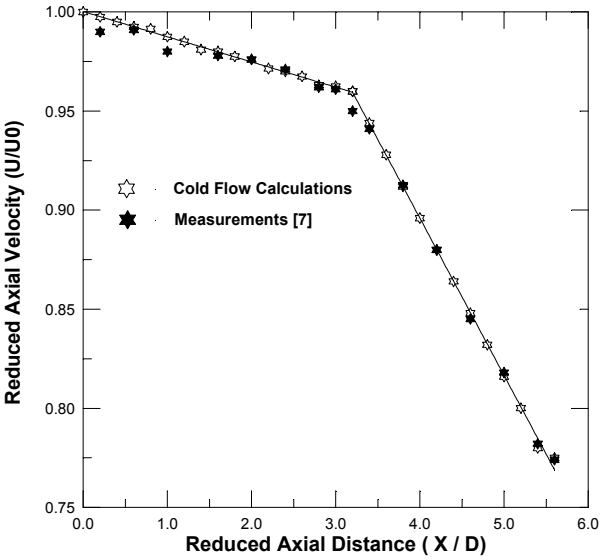

Fig. 7. Axial velocity profile along the chamber centerline.

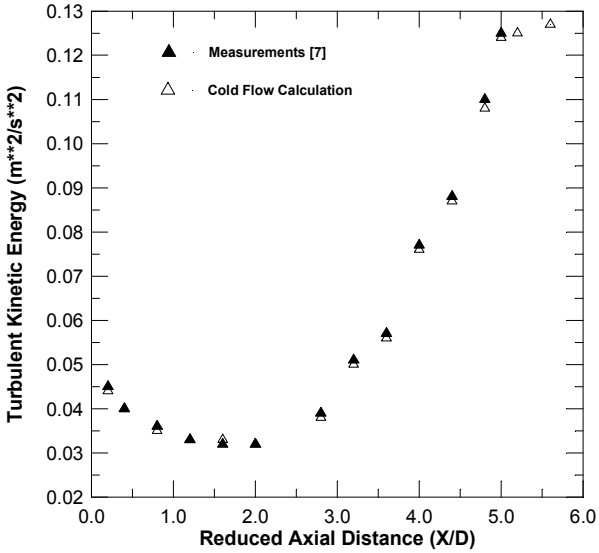

Fig. 8. Centerline profile of the turbulent kinetic energy.

This behavior is due to the training effect characterized by an important momentum transfer from the jet to its surrounding. As the jet develops axially, the mixing zone thickens and eventually reaches the axis while affecting the centerline velocity. Good agreement is observed between numerical and experimental values. Moreover, the axial distance $X/D \approx 3.1$ (where the slope change is noticed) is quite close to the value ($X/D = 3.0$) measured by Lachaux [7]. Predicted values of the mean turbulent kinetic energy at various axial stations (Fig. 8) seem to fit well the experimental measurements despite a slight underestimation of 7% noticed downstream the axial location X/D = 3.1. The discrepancy is certainly due to the isotropy of the turbulent stresses considered in the formulation of the ($k-\varepsilon$) model.

5.4 Partially premixed combustion

The study is performed in the case of a large-scale stratified condition where the equivalence ratio ranges from $\Phi = 1.03$ for the hot co-flow to $\Phi = 0.6$ for the main flow.

In this case, one follows the practice relevant to fully premixed situations and introduces a "pseudo" progress variable $\tilde{c} = 1 - \tilde{Y}/\tilde{\xi}$ that accounts for both fuel consumption and mixing rate. The previous definition of $\tilde{c}$ (denoted progress variable in the following) is valid for both fuel-lean and near-stoichiometric situations of partially premixed flames [28]. Accordingly, $\tilde{c} = 0$ within the fresh mixture and $\tilde{c} = 1$ in the burnt gases. The mean flame front is believed to be located in the region where the progress variable $\tilde{c}$ ranges between zero and unity. Regarding the flow dynamics, centerline profiles for the mean velocity component $\tilde{u}$ and the turbulent kinetic energy $\tilde{k}$ are illustrated on Figs. 9(a) and 9(b) respectively. In the upstream of the flame front (Fig. 9(a)), the slope of the axial velocity is quite similar to that for the non reactive case. The tendency is different when approaching the reaction zone. Indeed, the isobaric character of the combustion yields an acceleration of the fresh gases right before the potential core region. Globally, the calculated profile of the axial velocity is in good agreement with the measurements [7]. The LW-P model allows a quite good prediction of the acceleration across the mean flame brush. However, the numerical profile of the turbulent kinetic energy is less accurate. Compared with the measurements, our calculation shows a relative underestimation up to 26% downstream the flame brush (Fig. 9(b)). The important decrease in the numerical values of $\tilde{k}$ is certainly due to the closure expressions of the scalar turbulent fluxes given in Eqs. (20) and (21).

Indeed, gradient approximations express a proportionality between turbulent fluctuations and mean flow gradients (within large structures). Therefore, they cannot account for flame generated turbulence that occurs within small structures [23].

Regarding the flame structure, limiting values for $\tilde{c}$ are clearly shown in the spatial contour depicted in Fig. 10(a).

The mean flame seems to be stabilized over the burner lips and exhibits a typical conical shape. Along the chamber centerline, the evolution of the mean progress variable agrees well the measurements (Fig. 10(b)) although the experimental curve is slightly steeper than the numerical one. As it was found by Robin et al. [28], the mean flame is most probably thicker than the experimental flame. This discrepancy is due to the gradient assumption considered on the scalar turbulent fluxes $\overline{\rho u'' Y''}$ (Eq. (21)).

In the same context, maximum thickness δ_F of the conical flame can be evaluated by analyzing the centerline evolution of the mean progress variable. As pointed out by Robin et al. [28], this quantity is defined as the axial distance for which $\tilde{c}$ increases from 0.01 to 0.99.

According to the centerline profile of $\tilde{c}$ (Fig. 10(a)) the calculated value $\delta_F = 62.5$ is slightly greater than the experimental one [7]. The corresponding relative deviation of

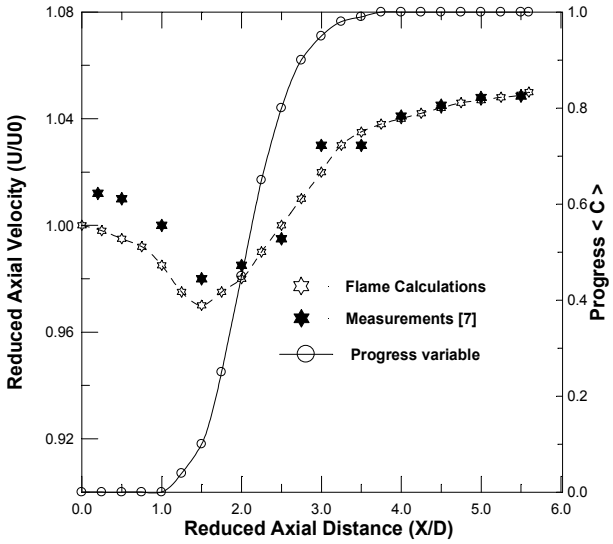

(a)

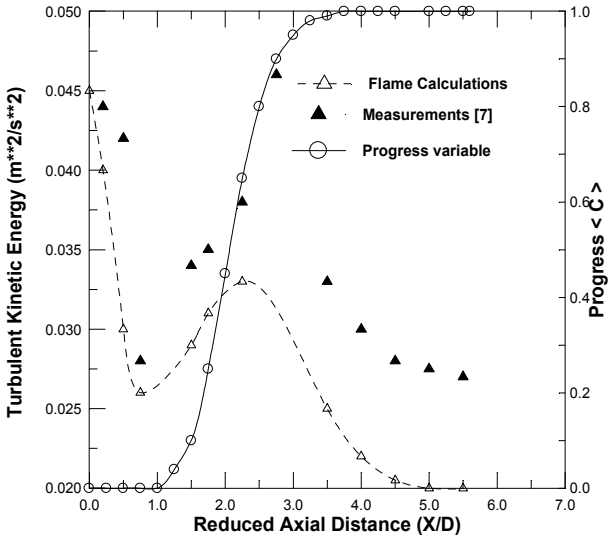

(b)

Fig. 9. (a) Velocity evolution along the chamber centerline; (b) Turbulent kinetic energy evolution along the chamber centerline.

11% confirms that the mean flame is thicker than the real flame.

A way of evaluating the ability of the LW-P model to recover the flame structure consists in comparing the evolution of the mean progress variable within the flame brush with the classical statements of Lipatnikov and Chomiak [29].

As pointed by these authors, the axial profile of the progress variable may be represented by a general exponential form [29]:

$$\tilde{c} = \frac{1}{1 + e^{-a\zeta}} \tag{32}$$

where a is a constant and ζ is a reduced spatial coordinate, defined as [29]:

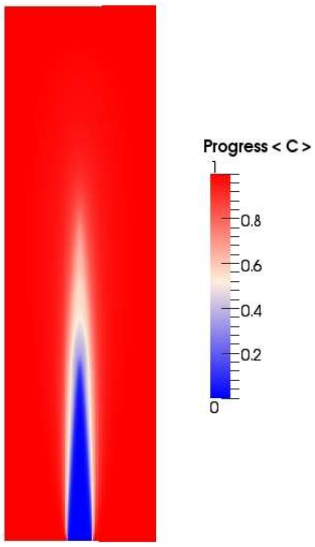

(a)

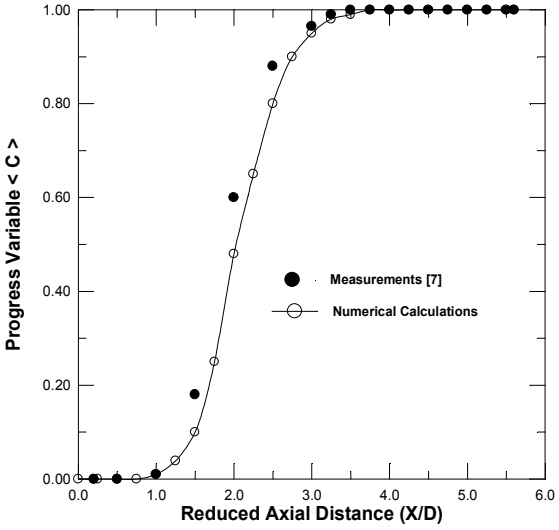

(b)

Fig. 10. (a) Spatial contour of the mean progress variable; (b) Axial evolution of the mean progress variable.

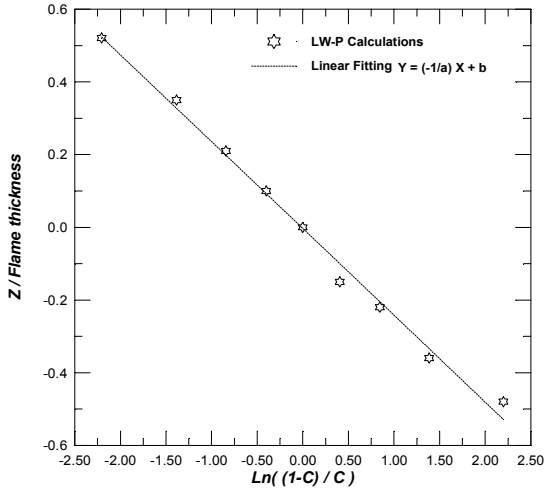

Fig. 11. Progress variable profile across the mean flame brush.

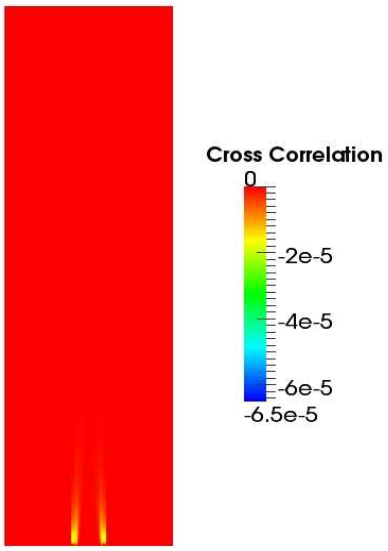

Fig. 12. Spatial contour of the cross-correlation.

$$\zeta = \frac{X - X_{\tilde{c}=0.5}}{\delta_F}. \tag{33}$$

Across the mean flame brush (centered at $\tilde{c} = 0.5$), the evolution of ζ with the quantity $Ln((1-\tilde{c})/\tilde{c})$ is depicted in Fig. 11. Here, a linear tendency with a constant slope $-1/a$ is noticed. It is calculated by means of a least square method. The obtained value $a = 4.20$ for the constant agrees quite well the measurement-based predictions of Pavé ($a = 4.28$) [5] and Shepherd $a = 4.02$ [6]. It appears that the evolution of iso-$\tilde{c}$ values within the mean flame brush can be well represented by a general curve which seems to be fairly universal.

As the LW-P solves the transport equations for the variances, it is interesting to take a look at the spatial distribution of the cross-correlation between the fuel mass fraction and the mixture fraction. The transported quantity $\overline{\rho Y'' \xi''} / \bar{\rho}$ results from the competition between mixing at small scales and chemical reactions within the definition domain D. As shown in Fig. 12, the cross-correlation is zero throughout the entire computational domain except in a restricted zone where it exhibits negative values. This can be explained as follows. Dealing with a lean mixture of reactants, the burnt gases are deprived from fuel ($Y = 0$) and this, whatever the value of the mixture fraction. Consequently, zero values for the cross-correlation are noticed in the burnt gases region. Moreover, in the upstream of the flame front the fresh gases were believed to be fully premixed (with a constant $\Phi = 0.6$) so that no fluctuations of the fuel mass fraction are encountered $\rho Y''^2 = 0$.

This also justifies the zero values for the cross-correlation within the fresh gases region. However negative values of the cross-correlation appear to be restricted in a region at the vi-

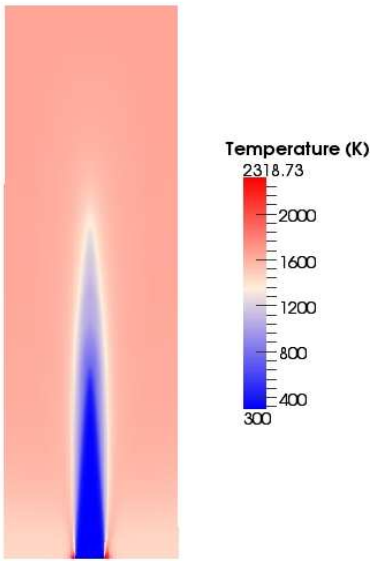

(a)

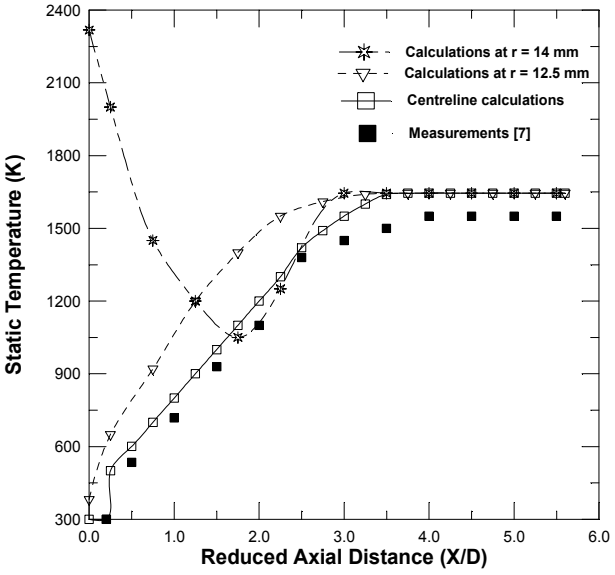

(b)

Fig. 13. (a) Spatial contour of the static temperature; (b) Static temperature profiles at various radial locations.

cinity of the co-flow inlet. The cross-correlation $\overline{\rho Y'' \xi''} / \overline{\rho}$ is more likely driven by the chemical process (where fuel is consumed) near the quasi-stoichiometric conditions resulting in the negative values sketched in Fig. 12.

Regarding the thermal level within the chamber, Fig. 13(a) depicts the spatial contour of the mean static temperature. It can be shown that the thermal contour zone of the mean flame exhibits a conical shape which is a typical configuration for a Bunsen flame. It is also noticed that the co-flow inlet is the hottest location of the combustion chamber.

This result was expected since the co-flow mixture was burned at quasi-stoichiometric conditions, yielding a localized peak (2,318 K) for the static temperature.

However, the co-flow does not seem to affect the thermal level within the chamber. The burnt gases are globally at a lower temperature (1,645 K) comparing with the co-flow's.

In the same context, Fig. 13(b) shows the static temperature profiles along the chamber axis at three radial locations, the centerline ($r = 0$), the burner lips ($r = 12.5$ mm) and the mid-entrance of the co-flow ($r = 14$ mm). The centerline profile of the static temperature increases gradually from the fresh gases value (300K) to reach the burnt gases temperature (1,645 K). Here an asymptotic tendency is noticed downstream the axial location *X/D* = 3.5 where reactions seem to be complete $\tilde{c} = 1$ (see Fig. 10(b)). As shown in Fig. 13(b), the numerical profile of the static temperature along the chamber centerline ($r = 0$) exhibits a good agreement with the measurements despite a maximum overestimation of 6% noticed in the burnt gases region. This discrepancy is certainly due to the global reaction modeling adopted in the chemistry description.

Indeed, the LW-P model considers only carbon dioxide CO_2 and water vapor H_2O as final products for the methane-air reaction and does not account for enthalpy losses by dissociation.

The behavior of the numerical profile in the vicinity of the burner lips ($r = 12.5$ mm) is almost similar to that along the chamber centerline. A slightly higher temperature is noticed upstream the asymptotic region. This is probably due to heat diffusion from the reaction zone to its neighboring. Moreover, the burnt gases temperature is reached from a distance *X/D* = *3.2* which is less than that observed for the centerline profile. The axial extent of the fresh gases is therefore decreasing radially with the distance from the chamber centerline. This behavior further confirms the conical shape of the mean flame.

6. Conclusions

A modeling and numerical study have been performed on a premixed pilot-stabilized methane-air flame. The LW-P model based on a two-scalar (Y, ξ) four delta Pdf was used to describe mixing and reaction progress within the burner-chamber device.

In the non reactive case, the Pope correction has allowed a good agreement with the experimental data, especially for the axial velocity and the turbulence decay prediction.

In the reactive case, a stabilization of the main flame was obtained thanks to the boundary conditions values adopted for the co-flow. The temperature measurements were locally overestimated by only 6% while the thermal level within the chamber was not affected. Spatial contour of the progress variable has clearly shown the conical shape of the mean flame. However, it was shown that the present version of the LW-P model does not improve the prediction of turbulent kinetic energy downstream of the flame brush. The numerical depletion observed on the mean turbulent kinetic energy is due to the use of the first order model ($k - \varepsilon$) which does not take into account the combustion induced turbulence.

Some efforts are still necessary to improve the turbulent

mixing by a full second-order model. Such a model will allow us to deal with the flame-generated turbulence due to counter-gradient diffusion in partially premixed conditions. Moreover, the extension of the model to include detailed chemistry effects still remains a challenging task.

Acknowledgment

The authors of the present paper would like to thank V. Robin, M. Champion and A. Mura from Pprime Institute at ENSMA-Poitiers France for their helps.

References

[1] D. Lee , J. Park, J. Jin and M. Lee, Simulation for prediction of nitrogen oxide emissions in lean premixed combustor, *The Journal of Mechanical Science and Technology,* 25 (7) (2011) 1871-1878.

[2] A. M. Elbaz, Early structure of LPG partially premixed conically stabilized flames, *Experimental Thermal and Fluid Science,* 44 (2013) 583-591.

[3] P. C. Vena and B. Deschamps, G. J. Smallwood and M. R. Johnson, Equivalence ratio gradient effects on flame front topology in a stratified iso-octane/air turbulent V-flame, *Proceedings of the Combustion Institute*, 33 (1) (2011) 1551-1558.

[4] Y. Dong, C. M. Vagelopoulos, C. M. Spedding, and F. N. Egolfopoulos, Measurement of laminar flame speeds through digital particle image velocimetry: mixtures of methane and ethane with hydrogen, oxygen, nitrogen and helium, *29th Symp. (Int.) on Combust*, 18 (2002) 1419 -1426.

[5] D. Pavé, Contribution to study the structure of a lean premixed turbulent methane-air flame, *Ph.D. thesis*, ICARE Institute, Orléans, France (2002).

[6] I. G. Shepherd, Flame surface density and burning rate in premixed turbulent flames, *26th Symposium (International) on Combustion*, *The Combustion Institute* (1996) 373-379.

[7] T. Lachaux, Pressure effects on the structure and dynamics of lean premixed turbulent methane-air flames, *Ph.D. thesis*, ICARE Institute, Orléans, France (2004).

[8] N. Jamsran and O. Taeck, A numerical analysis of the effects of a stratified pre-mixture on homogeneous charge compression ignition combustion, *The Journal of Mechanical Science and Technology,* 26 (6) (2012) 1929-1935.

[9] R. Adnan, H. H. Masjuki and T. M. I. Mahlia, Mathematical modeling on the effect of equivalence ratio in emission characteristics of compression ignition engine with hydrogen substitution, *Applied Mathematics and Computation,* 217 (13) (2011) 6144-6158.

[10] N. S. Park and S. C. Ko, Large eddy simulation of turbulent premixed combustion flow around bluff body, *The Journal of Mechanical Science and Technology,* 25 (9) (2011) 2227-2235.

[11] F. Zhang, R. Yu and X. S. Bai, Detailed numerical simulation of syngas combustion under partially premixed combustion engine conditions, *International Journal of Hydrogen Energy,* 37(22) (2012) 17285-17293.

[12] J. Helie and A. Trouvé, A modified coherent flame model to describe turbulent flame propagation in mixtures with variable composition, *Proc. Combust. Instit,* 28 (2000) 193-201.

[13] S. Bondi and W. P. Jones, A combustion model for premixed flames with varying stoichiometry, *Proc. Combust. Instit* 29 (2002) 2123-2129.

[14] K. N. C. Bray, M. Champion and P. A. Libby, Bray-Moss thermochemistry revisited, *Combust. Sci. Technol,* 174 (7) (2002) 167-174.

[15] H. Kolla, H. Rogerson, N. Chakraborty and N. Swaminathan, Scalar dissipation rate modeling and its validation, *Combust. Sci. Technol,* 181 (2009) 518-535.

[16] P. Libby and F. Williams, A presumed Pdf analysis of partially premixed turbulent combustion, *Combust. Sci. Technol,* 161 (2000) 351-390.

[17] V. Robin, A. Mura, M. Champion and P. Plion, A multi-Dirac presumed pdf model for turbulent reactive flows with variable equivalence ratio, *Combust. Sci. Technol,* 178 (2006) 1843-1870.

[18] G. Ribert, M. Champion and P. Plion Modeling turbulent reactive flows with variable equivalence ratio: Application to the calculation of a reactive shear layer, *Combust. Sci. Technol,* 176 (2004) 907-923.

[19] V. Robin, A. Mura, M. Champion, O. Degardin, B. Renou and M. Boukhalfa, Experimental and numerical analysis of stratified turbulent V-shaped flames, *Combust. Flame.,* 153 (2008) 288-315.

[20] T. Poinsot and D. Veynante, *Theoretical and numerical combustion*, Second Ed. R. T. Edwards Editions, Philadelphia, PA, USA (2005).

[21] B. E. Launder and D. B. Spalding, The numerical computation of the turbulent flows, *Comput. Meth. Appl.Mech Eng,* 3, (1974) 269-289.

[22] E. Fernandez-Tarrazo, A. Sanchez, A. Linan and F. A. Williams, A simple one-step chemistry model for partially premixed hydrocarbon combustion, *Combust. Flame*, 147 (1-2) (2006) 32-38.

[23] V. Robin, A. Mura and M. Champion, Algebraic models for turbulent transports in premixed flames, *Combust. Sci. Technol,* 184 (2012) 1718-1742.

[24] D. B. Spalding, Mixing and chemical reaction in confined turbulent flames, *Chem. Eng. Sci.*, 26 (1971) 95-107.

[25] A. Mura, V. Robin and M. Champion, A second-order model for turbulent reactive flows with variable equivalence ratio, *Combust. Flame*, 149 (2007) 217-224.

[26] F. Archambeau, N. Mehitoua and M. Sakiz, A finite volume code for the computation of turbulent flows, *Int. J. Finite,* 1 (2004) 1-62.

[27] S. B. Pope, An explanation of the turbulent round-jet / plane-jet anomaly, *AIAA Journal,* 16 (3) (1978) 279-281.

[28] V. Robin, N. Guilbert, A. Mura and M. Champion, Turbulent combustion modeling of mixtures with inhomogeneous equivalence ratio: Application to a flame stabilized by the

sudden expansion of a 2-D channel, *C. R. Mecanique*, 338 (2010) 40-47.

[29] A. N. Lipatnikov and J. Chomiak, Turbulent flame speed and thickness: phenomenology, evaluation and application in multi-dimensional simulations, *Prog.Energ.Comb. Sci*., 28 (2002) 1-73.

Abdallah Benarous works as an associate professor at Hassiba Benbouali University of Chlef, Algeria. He is also considered as a permanent researcher at the LTE laboratory, ENP, Oran, Algeria. His present research interests turbulent combustion modeling and supercritical thermodynamics. He received his Ph.D. in the field of aero-mechanical engineering in 2010 at Oran University of Sciences and Technology (USTO) in partnership with ENSMA- Poitiers, France. He is currently working on scalar dissipation closure models regarding partially premixed flames. Since 2002, he has participated in several national and international meetings and scientific conferences.

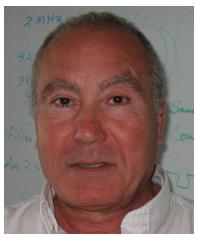

Djamel Karmed works as an associate professor at the ENSMA school, University of Poitiers, France. He is also considered as a permanent researcher at the ISAE Institute. His present research interests turbulent combustion as well as models implementation within the Code-Saturne solver. He is currently working on countergradient diffusion problems on partially premixed flames.

Abdelkrim Liazid is Professor and the head of the LTE Laboratory in ENP-Oran, Algeria. He works on the combustion and propulsion research area. He received his Ph.D. in the field of energy and heat transfer in 1993 at the Ecole Centrale- Lyon, France. He has published in various theoretical and applied scientific reviews and performs several works related to alternative fuels developments for internal combustion engines.